Research Article | Vol. 33, No. 8 / 21 Apr 2025 / Optics Express 17965
Optics EXPRESS

Sub-40-fs diode-pumped ytterbium-doped mixed rare-earth calcium oxoborate laser

HUANG-JUN ZENG,[1] ZHANG-LANG LIN,[1] HAIFENG LIN,[2] PAVEL LOIKO,[3] LIZHEN ZHANG,[1] ZHOUBIN LIN,[1] HSING-CHIH LIANG,[4] XAVIER MATEOS,[5] VALENTIN PETROV,[6] GE ZHANG,[1,7] AND WEIDONG CHEN[1,6,*]

[1]*State Key Laboratory of Functional Crystals and Devices, Fujian Institute of Research on the Structure of Matter, Chinese Academy of Sciences, 350002 Fuzhou, China*
[2]*Department of Physics, Umeå University, 901 87 Umeå, Sweden*
[3]*Centre de Recherche sur les Ions, les Matériaux et la Photonique (CIMAP), UMR 6252 CEA-CNRS-ENSICAEN, Université de Caen, 6 Boulevard Maréchal Juin, 14050 Caen Cedex 4, France*
[4]*Institute of Physics, National Yang Ming Chiao Tung University, 30010 Hsinchu, Taiwan*
[5]*Universitat Rovira i Virgili, URV, Física i Cristal·lografia de Materials, (FiCMA)- Marcel·lí Domingo 1, 43007 Tarragona, Spain*
[6]*Max Born Institute for Nonlinear Optics and Short Pulse Spectroscopy, Max-Born-Str. 2a, 12489 Berlin, Germany*
[7]*zhg@fjirsm.ac.cn*
[*]*chenweidong@fjirsm.ac.cn*

Abstract: We present a detailed comparative investigation of the continuous-wave and mode-locked laser performance of a mixed rare-earth calcium oxoborate crystal, Yb:(Gd,Y)$Ca_4O(BO_3)_3$, abbreviated as Yb:(Gd,Y)COB, for all three principal optical polarizations. Pumped by a low-power, single-transverse-mode, fiber-coupled laser diode at 976 nm, the Yb:(Gd,Y)COB laser generated soliton pulses as short as 32 fs at 1052.4 nm via soft-aperture Kerr-lens mode-locking, delivering an average output power of 51 mW at ~66.2 MHz for light polarization $\boldsymbol{E} \parallel \boldsymbol{Z}$. For light polarization $\boldsymbol{E} \parallel \boldsymbol{Y}$, slightly longer (34 fs) pulses were directly generated at 1053.7 nm, with a higher average output power of 86 mW at ~66.7 MHz. To the best of our knowledge, these results represent the shortest pulses ever achieved from any Yb^{3+}-doped borate crystal.

1. Introduction

Ytterbium (Yb^{3+})-doped rare-earth calcium oxoborates, Yb^{3+}:$RECa_4O(BO_3)_3$, where RE^{3+} denotes Y^{3+} [1], Gd^{3+} [2], or La^{3+} [3], represent a family of structurally disordered laser crystals characterized by relatively broad gain profiles, enabling sub-50 fs pulse generation in passively mode-locked (ML) lasers [4,5]. The Y-based compound is abbreviated as Yb:YCOB, and the Gd-based one as Yb:GdCOB. Both crystallize with monoclinic structure with the non-centrosymmetric space group *Cm*. Each RE^{3+} ion is coordinated by six O^{2-} anions, forming a distorted octahedron. The relatively large spacing between RE^{3+} ions and the similarity of ionic radii of VI-fold oxygen-coordinated RE^{3+} and Yb^{3+} allow for high doping levels in Yb:$RECa_4O(BO_3)_3$ crystals with minimal concentration quenching. The host crystals are optically biaxial and exhibit local structural disorder due to the random distribution of RE^{3+} and Ca^{2+} ions over two distorted octahedral sites. This disorder leads to inhomogeneous broadening of the dopant spectral lines in absorption and emission. Such crystals exhibit one of the largest splitting of the ground-state ($^2F_{7/2}$) Yb^{3+} manifold (>1000 cm^{-1}), which facilitates high-efficiency and low-threshold laser operation with minimal temperature sensitivity [6].

The non-centrosymmetric structures of the GdCOB and YCOB host crystals determine excellent second-order optical nonlinear properties [7], making them highly attractive for applications

#558581 https://doi.org/10.1364/OE.558581
Journal © 2025 Received 3 Feb 2025; revised 4 Apr 2025; accepted 5 Apr 2025; published 15 Apr 2025

Optics EXPRESS

in second-harmonic generation (SHG) [8] and optical parametric chirped pulse amplification (OPCPA) [9] especially due to the availability of larger sizes compared to other nonlinear borate crystals. Additionally, GdCOB and YCOB possess very high values of nonlinear refractive indices, measured at 11.4 cm^2/GW for GdCOB and 9 cm^2/GW for YCOB at 1.3 µm [10], which are particularly advantageous for ultrashort-pulse generation via Kerr nonlinearity in mode-locked (ML) lasers. The YCOB and GdCOB crystals also feature attractive thermo-optic properties [6,11]. When used as laser gain media for generating sub-100 fs pulses via passive mode-locking, Yb:GdCOB and Yb:YCOB have demonstrated remarkable performance. Using a high-finesse SESAM as a saturable absorber, a diode-pumped Yb:GdCOB laser has generated 90 fs pulses at 1045 nm with an average output power of 40 mW at 100 MHz [12]. The shortest pulses reported to date were achieved using an Yb:YCOB crystal: A diode-pumped laser employing a SEmiconductor Saturable Absorber Mirror (SESAM) as the mode-locking element generated 35 fs pulses at 1055 nm with a moderate average output power of 36 mW at ~95 MHz [13].

The structural disorder inherent to the $RECa_4O(BO_3)_3$ compounds can be further enhanced by introducing compositional disorder, leading to additional inhomogeneous spectral broadening, smoothing, and flattening of the gain spectral profiles of the Yb^{3+} ion. This effect has been demonstrated by mixing GdCOB and YCOB, where partial substitution of Y^{3+} by Gd^{3+} was realized in a composition with measured concentrations of 9.3 at.% Yb^{3+}, 23.5 at.% Gd^{3+}, and 67.2 at.% Y^{3+}. The resulting crystal, $Yb_{0.093}Gd_{0.235}Y_{0.672}Ca_4O(BO_3)_3$, abbreviated as Yb:(Gd,Y)COB, exhibited excellent laser properties in both continuous-wave (CW) and ML regimes [14–16]. Using a SESAM to facilitate soft-aperture Kerr-lens mode-locking (KLM), a diode-pumped Yb:(Gd,Y)COB laser generated near Fourier-limited soliton pulses as short as 43 fs at 1036.7 nm with an average output power of 84 mW at ~70.8 MHz [17].

Motivated by these promising spectroscopic properties and ML laser results, we further investigated the potential of Yb:(Gd,Y)COB for sub-40 fs pulse generation via soft-aperture KLM for the three principal optical polarizations. Employing a low-power, spatially single-mode, fiber-coupled laser diode at 976 nm as the pump source, we evaluated its CW laser performance, spectral tuning range, and KLM laser characteristics. The experimental results confirm the potential of this mixed crystal for generating ultrashort pulses with durations shorter than 40 fs and peak powers on the order of several tens of kilowatts.

2. Experimental setup

The layout of the diode-pumped Yb:(Gd,Y)COB laser employing an X-shaped, astigmatically compensated standing-wave cavity, as depicted in Fig. 1.

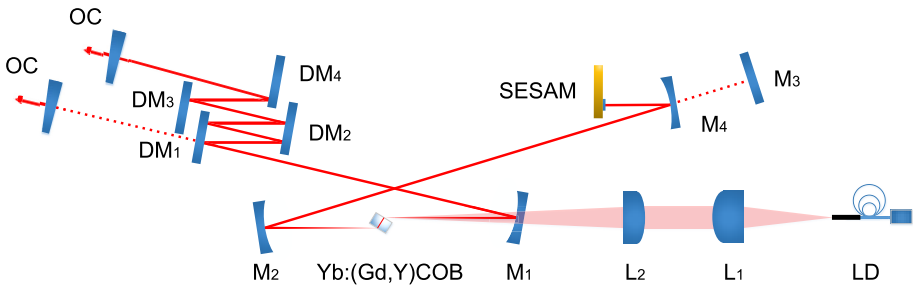

Fig. 1. Experimental setup of the diode-pumped Yb:(Gd,Y)COB laser. LD: fiber-coupled laser diode; L_1: aspherical lens; L_2: spherical lens; M_1, M_2 and M_4: concave mirrors; M_3: flat rear mirror for CW laser operation; DM_1 – DM_4: flat dispersive mirrors; OC: output coupler; SESAM: SEmiconductor Saturable Absorber Mirror.

Optics EXPRESS

The pump source was a single-transverse-mode, fiber-coupled InGaAs laser diode that emitted unpolarized radiation with a maximum incident power of 1.29 W at 976 nm. The emission wavelength was stabilized using a fiber Bragg grating (FBG), ensuring a spectral linewidth of ~0.2 nm (full width at half maximum, FWHM). The laser diode delivered a nearly diffraction-limited beam with a propagation factor (M^2) of ~1.02 at maximum power. The pump beam was collimated by an aspherical lens (L_1, focal length: $f = 26$ mm) and then focused into the laser crystal through the pump mirror (M_1) using a spherical lens ($L_2, f = 75$ mm). This setup produced a beam waist (radius) of 18.9 μm in the sagittal plane and 36.8 μm in the tangential plane (on the crystal). The optical and spectroscopic properties of the biaxial Yb:(Gd,Y)COB crystal are characterized in the frame of the optical indicatrix, which defines three mutually orthogonal principal axes: ***X***, ***Y***, and ***Z***, with refractive indices satisfying the relation $n_x<n_y<n_z$. Two uncoated samples, each with an Yb^{3+} doping concentration of 9.3 at.%, a thickness of 3.5-mm, and an aperture of 4×4 mm^2, were cut from the same as-grown bulk crystal for light propagation along the ***Y***-axis (***Y***-cut) and ***Z***-axis (***Z***-cut). By appropriately orienting the samples at Brewster's angle, the diode-pumped Yb:(Gd,Y)COB laser emitted linearly polarized radiation along the three principal axes. The crystals were mounted in copper holders without active cooling and positioned between two concave folding mirrors (M_1 and M_2) with a radius of curvature (RoC) of -100 mm.

The CW laser performance of the Yb:(Gd,Y)COB crystals was evaluated using a four-mirror cavity without saturable absorber and dispersive mirrors (DMs), and characterized for the three principal polarizations (see Fig. 1). The cavity design incorporated a flat rear mirror (M_3) in one arm and a plane-wedged output coupler (OC) in the other, with selectable OC transmission (T_{OC}) ranging from 0.6% to 10%. Using the ray transfer matrix (ABCD) formalism, the cavity mode within the crystal was calculated, yielding beam waist (radius) of 21 μm in the sagittal plane and 37 μm in the tangential plane. This indicates a well optimized mode-matching efficiency.

For ML laser operation, four flat DMs (DM_1 - DM_4) were used to compensate for the material dispersion and balance the self-phase modulation (SPM) induced by the Kerr nonlinearity of the laser crystal. A total negative round-trip group delay dispersion (GDD) of -1620 fs^2 was introduced by applying two bounces on DM_1 (GDD = -55 fs^2 per bounce) and DM_2 (GDD = -100 fs^2 per bounce), along with one bounce on DM_3 (GDD = -250 fs^2 per bounce) and DM_4 (GDD = -250 fs^2 per bounce). A commercial SESAM (BATOP, GmbH), featuring a modulation depth of 1.2%, a relaxation time of ~1 ps, and a non-saturable loss of ~0.8% at ~1 μm was employed to initiate and stabilize KLM operation. The second cavity beam waist was created on the SESAM by a concave mirror, M_4 (RoC = -100 mm), resulting in a beam radius of ~80 μm. The physical cavity length for the ML laser configuration was ~2.25 m, corresponding to a pulse repetition rate of ~66.5 MHz.

3. Continuous-wave laser performance

The ***Y***-cut sample was first used to investigate the CW laser performance of the Yb:(Gd,Y)COB crystal for light polarization with ***E*** || ***X***. The CW output power as a function of absorbed pump power for different T_{OC} values is shown in Fig. 2(a). Under lasing conditions, the measured pump absorption exhibited a slight reduction from 65.9% to 60% as the OC transmission (T_{OC}) increased from 0.6% to 10%. This reduction was attributed to the diminishing population recycling effect at lower intracavity intensity. Using a 4% OC, the diode-pumped Yb:(Gd,Y)COB laser produced a maximum CW output power of 481 mW for light polarization ***E*** || ***X*** at an absorbed pump power of 846 mW, corresponding to a slope efficiency (η) of 62.2% and a laser efficiency of $\eta_{laser} = 56.9\%$. The maximum $\eta = 65.8\%$ was obtained with a 10% OC at 1032.6 nm, corresponding to a CW output power of 429 mW at an absorbed pump power of 772 mW. The laser threshold in the CW regime increased with T_{OC}, ranging from 26 mW (T_{OC} =0.6%) to 112 mW ($T_{OC} = 10\%$). The emission wavelength of the diode-pumped Yb:(Gd,Y)COB laser

Optics EXPRESS

exhibited a gradual blue-shift with T_{OC}, shifting from 1083.3 to 1032.6 nm as T_{OC} increased from 0.6% to 10%. This behavior is characteristic of quasi-three-level Yb lasers with intrinsic reabsorption at the laser wavelength.

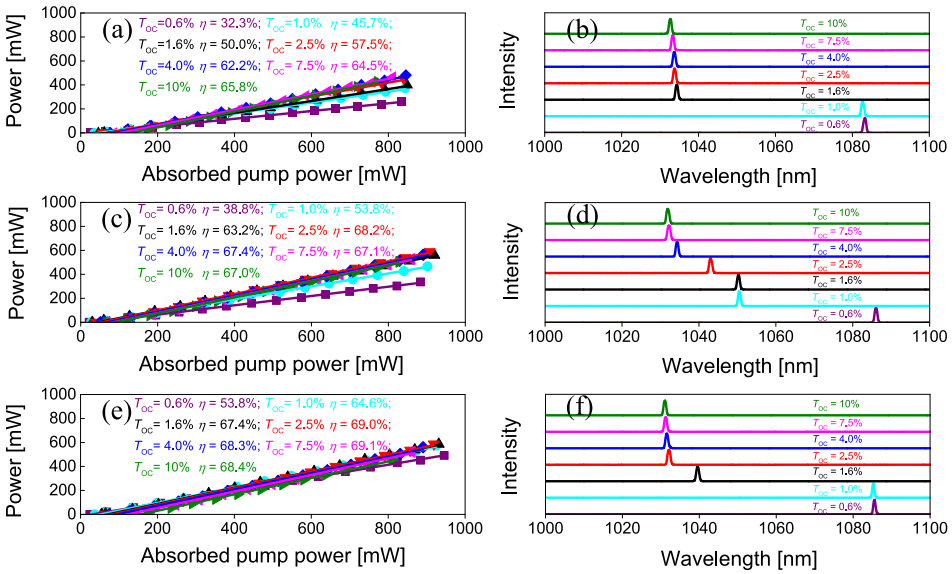

Fig. 2. Diode-pumped CW Yb:(Gd,Y)COB laser: (a,c,e) power transfer curves for different T_{OC}; (b,d,f) laser spectra. Crystal cut and laser polarization: (a,b) ***Y***-cut, ***E*** || ***X***; (c,d) ***Y***-cut, ***E*** || ***Z***; (e,f) ***Z***-cut, ***E*** || ***Y***.

The same ***Y***-cut sample was then oriented to ensure that the laser polarization was ***E*** || ***Z***. The measured pump absorption under lasing conditions showed a similar dependence on T_{OC}, varying from 71.4% to 64% as T_{OC} increased from 0.6% to 10%. The input-output characteristics of the diode-pumped CW Yb:(Gd,Y)COB laser for ***E*** || ***Z*** are presented in Fig. 2(c). Using a 2.5% OC, the maximum CW output power reached 588 mW at an absorbed pump power of 908 mW, corresponding to a $\eta = 68.2\%$ and $\eta_{laser} = 64.8\%$. The laser threshold increased with T_{OC}, ranging from 22 mW (T_{OC} =0.6%) to 67 mW (T_{OC} = 10%). The laser emission wavelength in the CW regime, shown in Fig. 2(d), exhibited a similar monotonic blue shift with increasing T_{OC}, ranging from 1086.1 nm ($T_{OC} = 0.6\%$) to 1031.9 nm ($T_{OC} = 10\%$).

Finally, the ***Z***-cut sample was used to investigate the CW laser performance of the Yb:(Gd,Y)COB crystal for light polarization ***E*** || ***Y***. The measured pump absorption under lasing conditions, varied from 73.4% to 62.9% as T_{OC} increased from 0.6% to 10%. The input-output characteristics for ***E*** || ***Y*** are presented in Fig. 2(e). Using a 2.5% OC, a maximum CW output power of 587 mW was achieved at an absorbed pump power of 919 mW, corresponding to $\eta = 69\%$ and $\eta_{laser} = 63.9\%$. The laser threshold increased with T_{OC}, ranging from 24 mW ($T_{OC} = 0.6\%$) to 142 mW ($T_{OC} = 10\%$). The laser wavelength exhibited again blue shift from 1085.5 nm (T_{OC} = 0.6%) to 1031 nm (T_{OC} = 10%), as shown in Fig. 2(f).

Following the Caird analysis [18], the total round-trip loss (δ) and the intrinsic slope efficiency (η_0), which accounts for the mode-matching efficiency and the quantum efficiency, were determined by fitting the measured slope efficiency η as a function of R_{OC}, where $R_{OC} = 1 - T_{OC}$ denotes the reflectivity of the OC, as shown in Fig. 3. The analysis revealed high intrinsic slope efficiencies of $\eta_0 = 75.5 \pm 1\%$ [see Fig. 3(a)], $78.7 \pm 3\%$ [see Fig. 3(c)], and $76.7 \pm 2\%$ [see Fig. 3(e)], along with low resonator losses of $\delta = 0.6 \pm 0.06\%$ [see Fig. 3(b)], $0.4 \pm 0.1\%$ [see Fig. 3(d)], and $0.2 \pm 0.04\%\%$ [see Fig. 3(f)] for light polarizations ***E*** || ***X***, ***E*** || ***Z***, and ***E*** || ***Y***,

Optics EXPRESS

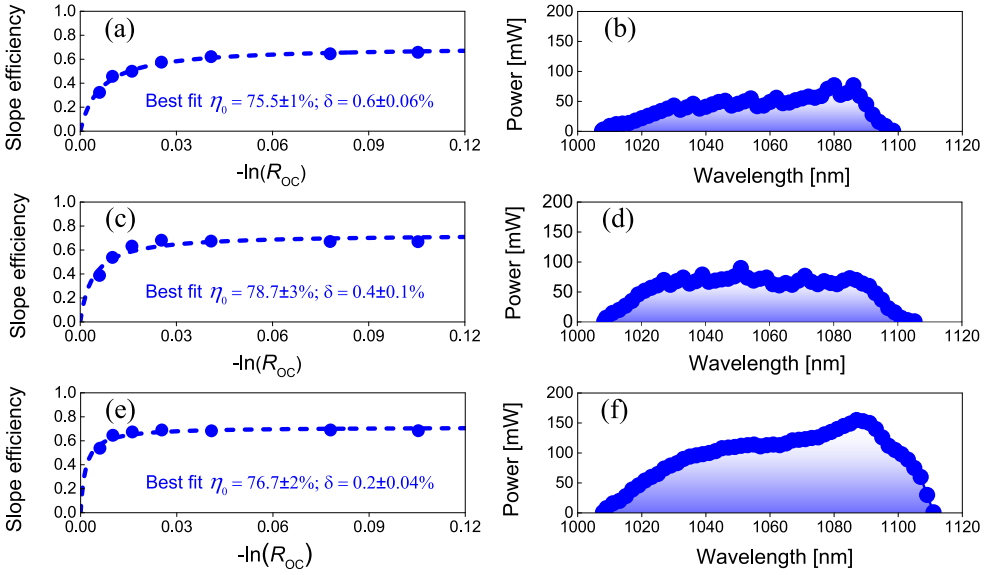

Fig. 3. Diode-pumped CW Yb:(Gd,Y)COB laser: Caird analysis for assessing the total round-trip cavity losses (δ) and the intrinsic slope efficiency (η_0). Crystal cut and laser polarization: (a) ***Y***-cut, ***E*** || ***X***; (c) ***Y***-cut, ***E*** || ***Z***; (e) ***Z***-cut, ***E*** || ***Y***; and laser wavelength tuning curves obtained using a quartz-based Lyot filter and a 0.2% OC. Crystal cut and laser polarization: (b) ***Y***-cut, ***E*** || ***X***; (d) ***Y***-cut, ***E*** || ***Z***; (f) ***Z***-cut, ***E*** || ***Y***.

respectively. The low values of δ indirectly confirm the excellent optical quality of the laser crystal.

The CW wavelength tuning of the diode-pumped Yb:(Gd,Y)COB laser was investigated by inserting a quartz-based Lyot filter at Brewster's angle near the OC (T_{OC} = 0.2%), as shown in Fig. 3. The emission wavelength of the laser was continuously tunable between 1008 - 1099 nm [***E*** || ***X***, see Fig. 3(b)], 1007 - 1105 nm [***E*** || ***Z***, see Fig. 3(d)] and 1008 - 1111 nm [***E*** || ***Y***, see Fig. 3(f)] covering a range of 91 nm, 98 nm and 103 nm, respectively, at the zero-power level and at the maximum incident pump power. Thus, light polization ***E*** || ***Y*** showed the broadest tuning range in the CW regime among all three principal light polarizations.

The results of CW laser operation for the three principal light polarizations using 3.5 mm thick samples are summarized in Table 1.

Up to the maximum applied pump power, corresponding to an absorbed power of 919 mW for ***E*** || ***Y***, see Fig. 2(e), the output power remained linearly proportional to the absorbed pump power, indicating no thermal issues. A maximum output power of 588 mW was achieved with T_{OC} = 2.5% for ***E*** || ***Z*** at an absorbed pump power of 908 mW. The maximum slope efficiency of 69.1%, with respect to the absorbed pump power, was obtained for ***E*** || ***Y*** using a 7.5% OC, while the highest laser efficiency of 64.8% was achieved for ***E*** || ***Z*** with a 2.5% OC. Compared to the parent Yb:YCOB crystal [4], the mixed Yb:(Gd,Y)COB crystal exhibits significantly broader spectral tuning curves for all three principal polarizations, making it highly promising for sub-40 fs pulse generation in different configurations.

Optics EXPRESS

Table 1. Characteristics[a] of the diode-pumped CW Yb:(Gd,Y)COB laser for the three principal polarizations

Yb:(Gd,Y)COB	$\boldsymbol{E} \parallel \boldsymbol{X}$	$\boldsymbol{E} \parallel \boldsymbol{Y}$	$\boldsymbol{E} \parallel \boldsymbol{Z}$
$P_{inc.}$ [W]	1.29	1.29	1.29
P_{abs} [mW]	846	919	908
P_{out} [mW]	481	587	588
P_{th} [mW] at $T_{OC} = 0.6\%$	26	24	22
T_{OC} *for max. power*	4%	2.5%	2.5%
η	62.2%	69%	68.2%
η_{laser}	56.9%	63.9%	64.8%
η_0	75.5%±1%	76.7%±2%	78.7%±3%
δ	0.6%±0.06%	0.2%±0.04%	0.4%±0.1%
Tuning range [nm]	91	103	98

[a] $P_{inc.}$ – maximum incident pump power, P_{abs} – maximum absorbed pump power, P_{out} – maximum output power, P_{th} – laser threshold, T_{OC} – transmission of output coupler, η – slope efficiency, η_{laser} – laser efficiency, η_0 – intrinsic slope efficiency, δ – total round-trip loss.

4. Kerr-lens mode-locked laser performance

For ML laser experiments, we used the same crystal cuts and the corresponding laser polarizations as described above. The diode-pumped Yb:(Gd,Y)COB laser was initially characterized at the maximum pump level for light polarization $\boldsymbol{E} \parallel \boldsymbol{X}$ using the $\boldsymbol{Y}$-cut sample and a 4% OC. By implementing a SESAM to stabilize and sustain soliton-like pulse shaping, soft-aperture KLM without any intracavity hard aperture could be readily achieved by adjusting the laser toward the edge of the cavity stability region. KLM operation was established by a slight knock on the OC or translating the SESAM. This led to an abrupt increase of the output power from 75 mW (CW regime) to 147 mW (ML regime). Under these situations, the optical spectrum of the laser pulses was centered at 1051.3 nm with a linewidth of 31.3 nm (FWHM) by assuming a sech^2-shaped spectral profile, see Fig. 4(a). The recorded background-free second-harmonic generation SHG-based intensity autocorrelation trace was almost perfectly fitted with a sech^2-shaped temporal profile, giving an estimated pulse duration of 39 fs (FWHM), see Fig. 4(b). The corresponding time-bandwidth product (TBP) of 0.330 was only slightly above the Fourier-transform-limited value (0.315). The measured absorbed pump power was 846 mW which corresponded to a laser efficiency of 17.4%. The calculated peak power was 49.1 kW at a pulse repetition rate of 67.6 MHz. The observed satellite peak around 1120 nm originated from the unmanageable intracavity GDD at the long-wave spectral wing and the non-optimized spectral reflectivity of the cavity mirrors. This phenomenon has already been observed in Yb:CALGO [19], and already explained by F. Druon *et al*. [20]. The effect could be suppressed by properly managing the total intracavity GDD over the full spectral bandwidth of the ML laser.

Soft-aperture KLM was further confirmed by monitoring the modification of the far-field beam profiles at transition from CW to the ML regime. An IR camera was placed at ∼1 m from the OC. The transition from CW to dominating soft-aperture KLM was accompanied by a significant shrinking of the beam diameter of the far-field, namely from 1.852 mm × 1.791 mm (CW) to 1.582 mm × 1.791 mm (ML), which is an evidence for a strong soft-aperture Kerr-lens effect and self-focusing inside the laser crystal, as shown in Fig. 5.

The shortest pulse duration for this polarization direction was obtained using a 1% OC. In this case, the Yb:(Gd,Y)COB laser emitted ultrashort pulses at a central wavelength of 1053.2 nm, with a spectral emission bandwidth of 35.2 nm (FWHM), assuming a sech^2-shape spectral

Optics EXPRESS

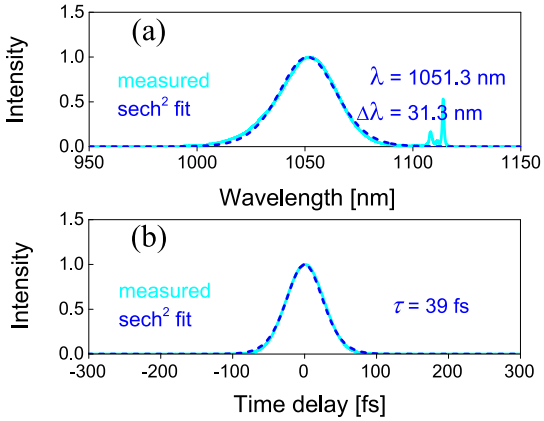

Fig. 4. Diode-pumped KLM Yb:(Gd,Y)COB laser with $T_{OC} = 4\%$. (a) Optical spectrum (*dashed curve* – sech^2 fit); (b) Intensity autocorrelation trace (*dashed curve* - sech^2 fit). Laser polarization: $\boldsymbol{E} \parallel \boldsymbol{X}$.

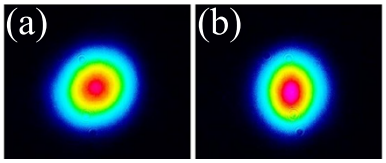

Fig. 5. Measured far-field beam profiles of the diode-pumped Yb:(Gd,Y)COB laser with 4% OC. (a) CW and (b) KLM regimes of operation.

profile, see Fig. 6(a). The recorded SHG-based intensity autocorrelation trace indicated a deconvolved pulse duration of 34 fs (FWHM), again assuming a sech^2-shaped temporal profile, see Fig. 6(b). The corresponding time-bandwidth product (TBP) was 0.323, still slightly above the Fourier-transform-limit (0.315), suggesting the presence of minimal residual chirp. A long-term autocorrelation scan (50 ps) confirmed steady-state single-pulse ML operation, as shown in the inset of Fig. 6(b). The shortest pulses were generated with at an average output power of 46 mW for an absorbed pump power of 844 mW, corresponding to a laser efficiency of 5.5% and a peak power of 17.6 kW.

Using the same $\boldsymbol{Y}$-cut sample with the same total round-trip negative GDD, KLM operation for $\boldsymbol{E} \parallel \boldsymbol{Z}$ delivered the shortest pulses also with a 1% OC. The measured optical spectrum exhibited an emission bandwidth of 39.8 nm (FWHM) and was centered at 1052.4 nm, see Fig. 6(c). The estimated pulse duration, derived from the recorded SHG-based intensity autocorrelation trace, was 32 fs (FWHM), see Fig. 6(d). The corresponding TBP of 0.345 was somewhat higher than the Fourier-transform limit, indicating some residual chirp. The shortest pulses were emitted at an average output power of 51 mW for an absorbed pump power of 902 mW, corresponding to a laser efficiency of 5.7% and a peak power of 21.2 kW. Although a narrow spectral feature appears near 1120 nm, long-range (50 ps) autocorrelation measurements showed no evidence of temporal pedestals or background emission. This confirms that the spectral feature does not translate into time-domain pulse degradation and is most likely a result of intracavity dispersion and mirror reflectivity characteristics at the spectral edge.

As in the CW regime, to access the light polarization $\boldsymbol{E} \parallel \boldsymbol{Y}$, we used the $\boldsymbol{Z}$-cut sample. The shortest pulses for this polarization were achieved with a 1.6% OC and the same GDD of -1620 fs^2, see Fig. 6. The emission spectrum was centered at 1053.7 nm and exhibited a bandwidth of 35 nm (FWHM), see Fig. 6(e). The deconvolved pulse duration was 34 fs (FWHM),

Optics EXPRESS

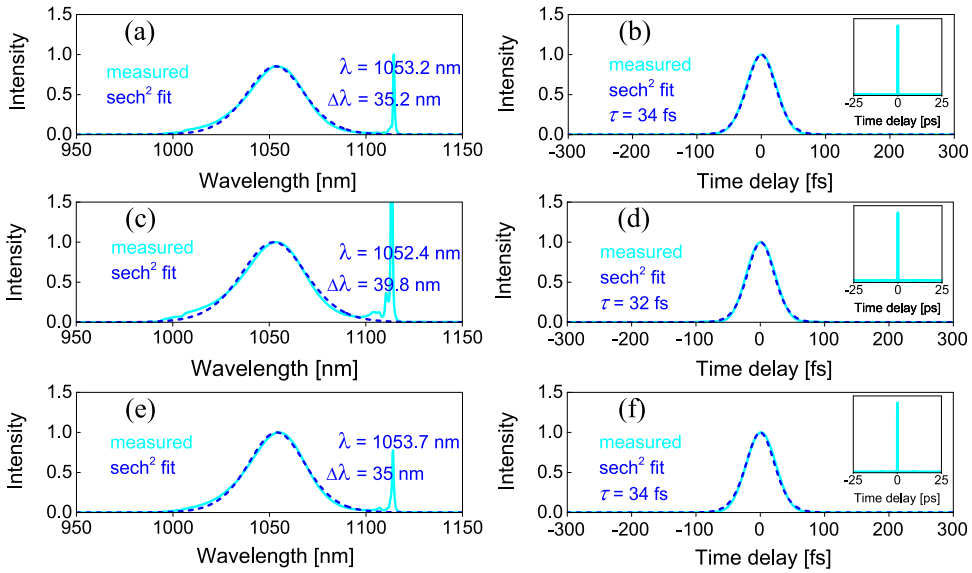

Fig. 6. Diode-pumped KLM Yb:(Gd,Y)COB laser. (a,c,e) optical spectra (*dashed curves* - sech^2 fits); (b,d,f) SHG-based intensity autocorrelation traces (*dashed curves* - sech^2 fits). *Insets*: autocorrelation traces measured over a time span of 50 ps. Crystal cut and laser polarization: (a,b) ***Y***-cut, ***E*** || ***X***, (c,d) ***Y***-cut, ***E*** || ***Z***; (e,f) ***Z***-cut, ***E*** || ***Y***. Output coupling: (a,b) 1%; (c,d) 1%; (e,f) 1.6%.

see Fig. 6(f), and the TBP of 0.321 was similar to that for ***E*** || ***X***. The average output power in this case was 86 mW at an absorbed pump power of 932 mW, corresponding to an optical efficiency of 9.2% and a peak power of 33.4 kW.

The radio frequency (RF) spectra of the shortest pulses were recorded to verify the stability of KLM operation across different frequency spans, as shown in Fig. 7. The fundamental repetition rate exhibited a high signal-to-noise ratio (SNR) of more than 76 dBc, with uniformly distributed harmonics recorded over a 1-GHz frequency span. These results confirm the high stability of the single-pulse ML operation, free from Q-switch instabilities, validating the robustness of the KLM mechanism.

For all three principal polarizations, sub-40 fs pulse durations were achieved from the KLM diode-pumped Yb:(Gd,Y)COB laser using 3.5 mm-thick samples and $T_{OC} = 4\%$ or less, as summarized in Table 2. This is an evidence for the excellent spectroscopic properties of this compositionally and structurally disordered crystal. The shortest pulses, with a duration of 32 fs, were generated at 1052.4 nm for light polarization with ***E*** || ***Z***. For the same polarization, the average output power of the diode-pumped KLM Yb:(Gd,Y)COB laser was scaled to 189 mW by employing a 4% OC, albeit at the cost of slightly longer pulse duration (35 fs). Our strictly comparative results for all polarizations confirm previous observations with Yb:YCOB [4,13] that for this family of crystal hosts polarization ***E*** || ***Z*** yields the best results. It should be outlined that this situation is optimum for self-frequency doubling operation based on the non-centrosymmetric nature of the lattice because phase-matching in the *X*-*Y* plane is possible for the fundamental wavelength in the 1-μm range based on *oo-e* negative type synchronism which means that the gain properties of the Yb^{3+}-ion will not be affected by the crystal cut satisfying the phase-matching condition.

Currently, Kerr-lens mode-locking is recognized as a principal tool for routinely generating sub-50 fs pulses directly out of an Ytterbium mode-locked oscillator. This progress was to a great extent enabled by the material engineering of crystalline gain media, namely, the control of

Optics EXPRESS

Table 2. Kerr-lens mode-locked performance[a] of the diode-pumped Yb:(Gd,Y)COB laser

T_{OC} [%]	P_{out} [mW]	P_{abs} [mW]	P_{peak} [kW]	η_{laser} [%]	τ [fs]	λ [nm]	$\Delta\lambda$ [nm]	TBP	Laser polarization
1.0	46	844	17.6	5.5%	34	1053.2	35.2	0.323	***E*** || ***X***
4.0	147	846	49.1	17.4%	39	1051.3	31.3	0.330	***E*** || ***X***
1.6	86	932	33.4	9.2%	34	1053.7	35.0	0.321	***E*** || ***Y***
4.0	141	891	47.7	15.8%	39	1053.4	32.4	0.341	***E*** || ***Y***
1.0	51	902	21.2	5.7%	32	1052.4	39.8	0.345	***E*** || ***Z***
4.0	189	891	71.8	21.2%	35	1050.8	34.9	0.332	***E*** || ***Z***

[a]T_{OC} – transmittance of the output coupler, P_{out} – average output power, P_{abs} – absorbed pump power, P_{peak} – peak power, η_{laser} – laser efficiency, τ – pulse duration (FWHM), TBP – time bandwidth product, λ – central emission wavelength, $\Delta\lambda$ – emission bandwidth (FWHM).

inhomogeneous spectral line broadening via compositional and / or structure disorder, resulting in smooth, structureless and flat gain profiles above 1 μm closely resembling those of laser glasses while maintaining reasonably good thermal properties of crystals (considering an inevitable drop in thermal conductivity in disordered compounds). Based on the model developed by Gaumé et al. [21], the thermal conductivity of the Yb:(Gd,Y)COB crystal used in this study (9.3% Yb, 23.5% Gd, 67.2% Y) is estimated to be reduced by approximately a factor of two compared to pure YCOB, i.e., from ~2 W/m·K to ~1 W/m·K. This decrease is an expected consequence of compositional disorder, which enhances spectroscopic broadening at the cost of thermal transport efficiency. Recently, we have achieved sub-40 fs pulses from KLM ytterbium lasers employing different crystals. In this regard, it is worth discussing the specific advantages of Yb^{3+}-doped oxoborates and in particular the studied mixed Yb:(Gd,Y)COB crystal. The parent compounds provide a unique combination of i) very high nonlinear refractive index n_2, ii) extremely large Yb^{3+} ground-state Stark splitting; iii) self-frequency doubling potential; iv) excellent thermal

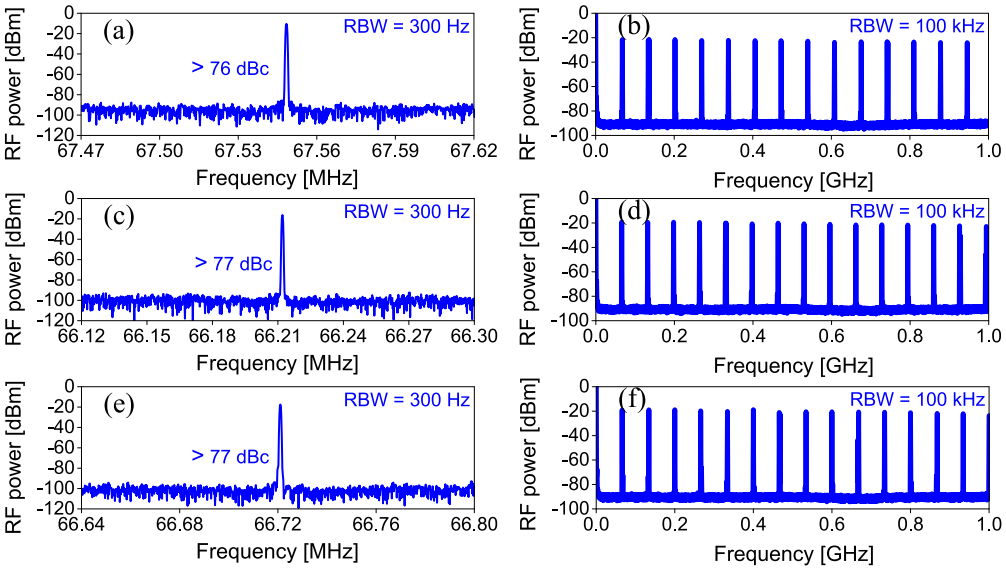

Fig. 7. RF spectra of the diode-pumped KLM Yb:(Gd,Y)COB laser: (a,c,e) Fundamental beat note, recorded with an RBW of 300 Hz; (b,d,f) Harmonics over a 1-GHz frequency span, recorded with an RBW of 100 kHz. Crystal cut and laser polarization: (a,b) ***Y***-cut, ***E*** || ***X***, (c,d) ***Y***-cut, ***E*** || ***Z***; (e,f) ***Z***-cut, ***E*** || ***Y***.

Optics EXPRESS

and thermo-optic properties; v) unlike many other Yb-doped gain media, the rare-earth calcium oxoborates belong to the class of non-centrosymmetric crystals, enabling direct self-frequency doubling. This makes them particularly attractive for applications requiring ultrashort pulses in the green part of the spectrum. These crystals seem unique with respect to short pulse durations in the green because they provide larger spectral gain bandwidths compared to the ordered Yb:YAB type non-centrosymmetric borate crystals [22–24]; vi) a strong electron-phonon interaction and vii) high Yb^{3+} doping levels enabling short interaction lengths. In this regard, lasers based on Yb^{3+}-doped parent and mixed (with additional spectral broadening) oxoborates can develop in two directions being unique among other Yb^{3+}-doped laser crystals employed so far (fluorides, sesquioxides, aluminates, *etc*.), namely, i) by exploiting their nonlinear properties for addressing femtosecond light sources in the visible and ii) by utilizing the long-wavelength vibronic (phonon-assisted) emission for pulse shortening at the fundamental wavelength and addressing the spectral range above 1.1 μm. The material engineering by admixing the Y^{3+}, Gd^{3+} and La^{3+} cations in the host matrix to tailor the spectral gain profiles, electron-phonon interaction and nonlinear properties is also promising.

5. Conclusion

In conclusion, we demonstrated sub-40 fs pulse generation from a diode-pumped Yb:(Gd,Y)COB laser via soft-aperture Kerr-lens mode-locking. In the present work, a commercial SESAM was employed to initiate and stabilize the mode-locked operation. Using a low-power, spatially single-mode, fiber-coupled InGaAs diode laser as the pump source, the Yb:(Gd,Y)COB laser generated soliton pulses as short as 32 fs at 1052.4 nm with an average output power of 51 mW for light polarization $\boldsymbol{E} \parallel \boldsymbol{Z}$. The maximum average output power of the sub-40 fs diode-pumped Yb:(Gd,Y)COB laser reached 189 mW with a slightly longer pulse duration of 35 fs, corresponding to a peak power of 71.8 kW and a laser efficiency of 21.2%. Thanks to the favorable thermo-mechanical and spectroscopic properties of the crystal, sub-40 fs pulses were directly generated from the diode-pumped KLM Yb-laser for all three principal polarizations. These results highlight the potential of Yb^{3+}-doped mixed oxoborate crystals, particularly with optimized Y^{3+}/Gd^{3+} ratios, for further power scaling and pulse shortening using the Kerr-lens mode-locking technique.

Funding. National Natural Science Foundation of China (62475263); Science and Technology Projects of Fujian Province (2024I0041, 2023H0047); Sino-German Scientist Cooperation and Exchanges Mobility Program (M-0040); European Social Fund Plus (2022FI_B200021, 2021FI_B100170, 2020FI_B00522); Ministerio de Ciencia, Innovación y Universidades (MICIU/AEI/10.13039/ 501100011033/ FEDER/UE).

Acknowledgment. Xavier Mateos acknowledges the Serra Húnter program.

Disclosures. The authors declare no conflicts of interest.

Data availability. Data underlying the results presented in this paper are not publicly available at this time but may be obtained from the authors upon reasonable request.

References

1. D. A. Hammons, J. M. Eichenholz, Q. Ye, *et al.*, "Laser action in Yb^{3+}:YCOB (Yb^{3+}:$YCa_4OBO_3)_3$)," Opt. Commun. **156**(4-6), 327–330 (1998).
2. F. Auge, F. Balembois, P. Georges, *et al.*, "Efficient and tunable continuous-wave diode-pumped Yb^{3+}:$Ca_4GdO(BO_3)_3$ laser," Appl. Opt. **38**(6), 976–979 (1999).
3. A. Aron, G. Aka, B. Viana, *et al.*, "Spectroscopic properties and laser performances of Yb:YCOB and potential of the Yb:LaCOB material," Opt. Mater. **16**(1-2), 181–188 (2001).
4. A. Yoshida, A. Schmidt, H. J. Zhang, *et al.*, "42-fs diode-pumped Yb:$Ca_4YO(BO_3)_3$ oscillator," Opt. Express **18**(23), 24325–24330 (2010).
5. Z. Y. Gao, J. F. Zhu, Z. M. Wu, *et al.*, "Tunable second harmonic generation from a Kerr-lens mode-locked Yb:$YCa_4O(BO_3)_3$ femtosecond laser," Chin. Phys. B **26**(4), 044202 (2017).
6. P. Loiko, J. M. Serres, X. Mateos, *et al.*, "Thermal lensing and multiwatt microchip laser operation of Yb:YCOB crystals," IEEE Photonics J. **8**(3), 1–12 (2016).

Optics EXPRESS

7. G. Aka, A. Kahn-Harari, F. Mougel, *et al.*, "Linear- and nonlinear-optical properties of a new gadolinium calcium oxoborate crystal, $Ca_4GdO(BO_3)_3$," J. Opt. Soc. Am. B **14**(9), 2238–2247 (1997).
8. J. Luo, S. J. Fan, H. Q. Xie, *et al.*, "Thermal and nonlinear optical properties of $Ca_4YO(BO_3)_3$," Cryst. Res. Technol. **36**(11), 1215–1221 (2001).
9. S. Yang, X. Liang, X. Xie, *et al.*, "Ultra-broadband high conversion efficiency optical parametric chirped-pulse amplification based on YCOB crystals," Opt. Express **28**(8), 11645–11651 (2020).
10. A. Major, J. S. Aitchison, P. W. E. Smith, *et al.*, "Z-scan measurements of the nonlinear refractive indices of novel Yb-doped laser crystal hosts," Appl. Phys. B **80**(2), 199–201 (2005).
11. P. Loiko, X. Mateos, Y. Wang, *et al.*, "Thermo-optic dispersion formulas for YCOB and GdCOB laser host crystals," Opt. Mater. Express **5**(5), 1089–1097 (2015).
12. F. Druon, F. Balembois, P. Georges, *et al.*, "Generation of 90-fs pulses from a mode-locked diode-pumped Yb^{3+}:$Ca_4GdO(BO_3)_3$ laser," Opt. Lett. **25**(6), 423–425 (2000).
13. A. Yoshida, A. Schmidt, V. Petrov, *et al.*, "Diode-pumped mode-locked Yb:YCOB laser generating 35 fs pulses," Opt. Lett. **36**(22), 4425–4427 (2011).
14. Y. Zhang, Z. Lin, Z. Hu, *et al.*, "Growth and spectroscopic properties of Yb^{3+}:$Gd_{0.5}Y_{0.5}Ca_4O(BO_3)_3$ crystal," J. Alloy Compd. **390**(1-2), 194–196 (2005).
15. Y. Zhang, B. Wei, and G. Wang, "Spectroscopic properties of Yb^{3+}-doped $Ca_4Gd_{0.5}Y_{0.5}O(BO_3)_3$ single crystals," Phys. Status Solidi A **207**(6), 1468–1473 (2010).
16. H. Lin, G. Zhang, L. Zhang, *et al.*, "SESAM mode-locked Yb:GdYCOB femtosecond laser," Opt. Mater. Express **7**(10), 3791–3795 (2017).
17. H. J. Zeng, H. Lin, Z. L. Lin, *et al.*, "Diode-pumped sub-50-fs Kerr-lens mode-locked Yb:GdYCOB laser," Opt. Express **29**(9), 13496–13503 (2021).
18. J. A. Caird, S. A. Payne, P. R. Staver, *et al.*, "Quantum electronic properties of the $Na_3Ga_2Li_3F_{12}$:Cr^{3+} laser," IEEE J. Quantum Electron. **24**(6), 1077–1099 (1988).
19. Y. Zaouter, J. Didierjean, F. Balembois, *et al.*, "47-fs diode-pumped Yb^{3+}:$CaGdAlO_4$ laser," Opt. Lett. **31**(1), 119–121 (2006).
20. P. Sévillano, P. Georges, F. Druon, *et al.*, "32-fs Kerr-lens mode-locked Yb:$CaGdAlO_4$ oscillator optically pumped by a bright fiber laser," Opt. Lett. **39**(20), 6001–6004 (2014).
21. R. Gaumé, B. Viana, D. Vivien, *et al.*, "A simple model for the prediction of thermal conductivity in pure and doped insulating crystals," Appl. Phys. Lett. **83**(7), 1355–1357 (2003).
22. S. Rivier, U. Griebner, V. Petrov, *et al.*, "Sub-90 fs pulses from a passively mode-locked Yb:$YAl_3(BO_3)_4$ laser," Appl. Phys. B **93**(4), 753–757 (2008).
23. P. Wang, P. Dekker, J. M. Dawes, *et al.*, "Efficient continuous-wave self-frequency-doubling green diode-pumped Yb:$YAl_3(BO_3)_4$ lasers," Opt. Lett. **25**(10), 731–733 (2000).
24. H. J. Zeng, Z. L. Lin, V. Petrov, *et al.*, "56-fs diode-pumped SESAM mode-locked Yb:$YAl_3(BO_3)_4$ laser," Opt. Express **31**(6), 10617–10624 (2023).